

EFFECTS OF MAGNETIZED WINDS ON ADVECTIVE DISKS. I. A SELF-SIMILAR SOLUTION

ROBERTO SORIA,^{1,2} JIANKE LI,² AND DAYAL T. WICKRAMASINGHE²

Received 1996 November 14; accepted 1997 May 8

ABSTRACT

In this paper we investigate the effects of a large-scale magnetic field (with open field lines) on the structure of an advective accretion disk. We find self-similar solutions to the MHD equations describing the disk/magnetic field system; these equations reduce to the case studied by Narayan & Yi (1994) in the absence of an external, macroscopic magnetic field. Our main assumptions are the existence of a hot, tenuous corona above and below the disk, and the presence of a wind starting from the base of the corona and centrifugally accelerated along the field lines up to the Alfvén surface. The wind appears to be the most efficient mechanism for extracting angular momentum from the inflowing gas, even when the mass lost in the wind is negligible with respect to the mass accreted; other notable effects of the interplay between the disk structure and the magnetic field with its associated wind include a bending of the field lines toward the surface of the disk (dragging of the field by the accreting matter), a squeezing effect (the disk scale height is reduced because of a magnetic pressure gradient), an increased radial infall velocity (consequence of the quicker loss of angular momentum), and a decrease of the gas temperature in the disk. We can equivalently describe the loss of angular momentum in the wind by introducing an effective viscosity parameter α_{eff} , which can become greater than 1 regardless of the true viscosity parameter α .

Subject headings: accretion, accretion disks — black hole physics — magnetic fields — MHD

1. INTRODUCTION

The standard model for accretion disks has been for many years the one developed by Shakura & Sunyaev (1973), Novikov & Thorne (1973), and Lynden-Bell & Pringle (1974). Its usefulness as a first approximation is well established, and the model is based on the simple assumption that at each radius the thermal energy generated by shear viscosity is immediately radiated away vertically: cooling processes can exactly balance the heating sources. As a consequence, the disk is geometrically thin, and the thermal energy of the gas much less than its orbital kinetic energy. Shear viscosity is also responsible for removing angular momentum from the gas during its infall, that is to say, for transferring angular momentum outward in the disk.

The natural improvement over the Shakura-Sunyaev (SS) model was to consider the case when cooling is less efficient than viscous heating. This may happen in two cases: either when the disk is extremely optically thick and the radiation is trapped for a timescale longer than the accretion timescale (see Abramowicz et al. 1988); or when it is extremely optically thin, a regime in which cooling processes are inefficient (Narayan & Yi 1995b). A simple, general model of “advective disk” was put forward by Narayan & Yi (1994, hereafter NY94; Narayan & Yi 1995a): they parameterized the degree of advection with one parameter f , defined as the ratio between the thermal energy “stored” in the disk and advected toward the central object (i.e., not reradiated), and the total thermal energy generated by viscosity, at each radius. The general result, obtained both from self-similar solutions and numerical calculations, is that high advection ($f \sim 1$) produces a hotter, thicker disk, with a larger infall

radial velocity and, conversely, a sub-Keplerian circular velocity.

Advective disks have sparked interest in the field, particularly since it appears that advective models can better fit the observational data of binary black hole candidates (see Narayan, McClintock, & Yi 1996; Narayan 1996) and low-luminosity active galactic nuclei (Narayan, Yi, & Mahadevan 1995; Lasota et al. 1996). An alternative model fitting the observations of BH candidates has been advocated by Ebisawa, Titarchuk, & Chakrabarti (1996), based on different physical processes, such as shocks and bulk-motion Comptonization (Chakrabarti & Titarchuk 1995).

In this paper we investigate the effect on the disk structure of a large-scale magnetic field threading the disk. The idea of an open magnetic field crossing the disk, and being dragged in by the inflow, was suggested by Blandford & Payne (1982), and it can explain the presence of winds and outflows from the disk surface: if the field lines are inclined at a sufficiently small angle from the disk plane, the gas can be centrifugally accelerated up to Alfvén speed and escape to infinity. A mechanism for launching, accelerating, and collimating gas outflows is invoked to justify the close link between winds or jets and accretion disks in astrophysics, necessary to explain the features of a variety of systems, from AGNs (e.g., Sun & Malkan 1989; Livio 1997) to CVs (e.g., Murray & Chiang 1996). The main effect of a magnetically driven wind will be to provide another mechanism for removing angular momentum from the accreting matter, in addition to viscous stress. Models accounting for this effect have been proposed by Lubow, Papaloizou, & Pringle (1994a, 1994b, hereafter LPP94), with an emphasis on the relation between angular momentum and mass losses in the outflow, and velocity of infall of the gas; and by Wardle & Königl (1993) in the case of weakly ionized protostellar accretion disks. In both cases, the disk is assumed to be nearly Keplerian and geometrically thin. A self-consistent set of self-similar solutions for a disk-wind system was derived by Li (1995), again in the thin disk approximation.

¹ Mount Stromlo and Siding Spring Observatories, Institute of Advanced Studies, Australian National University, Private Bag, Weston Creek Post Office, ACT 2611, Australia; roberto@mso.anu.edu.au.

² The Australian National University Astrophysical Theory Centre, Canberra, ACT 0200, Australia; ljk@maths.anu.edu.au, dayal@maths.anu.edu.au.

Following the example of these papers, we try here to apply a large-scale magnetic field with wind to advective disk models. We note that Narayan & Yi (1995b) do not consider this case: they only allow for an isotropically tangled magnetic field within the disk, behaving like radiation, i.e., contributing to the pressure and the internal energy with terms $\sim B^2 \sim \rho^{4/3}$. We assume in our model that the wind originates from a hot, tenuous corona above the disk. As far as the disk structure is concerned, we still use vertically integrated quantities, but we have to consider the case of geometrically thick, sub-Keplerian disks. In this paper we limit our treatment to self-similar solutions (all physical quantities scaling as powers of R according to their dimensions), similarly to NY94; despite some limitations, they can give a physically intuitive picture of the magnetic effects; more sophisticated numerical three-dimensional calculations are left to further work.

2. MAGNETIC DISK EQUATIONS

We assume a steady-state, axisymmetric flow; the fundamental equations that determine the disk structure are the continuity, momentum and induction equations (e.g., Campbell 1992a, 1992b), in Gaussian units with $c = 1$:

$$\nabla \cdot (\rho \mathbf{v}) = 0, \quad (1)$$

$$(\mathbf{v} \cdot \nabla) \mathbf{v} = -\frac{\nabla P}{\rho} - \nabla \phi + \frac{1}{\rho} \cdot (\mathbf{j} \times \mathbf{B} + \mathbf{F}_{\text{vis}}), \quad (2)$$

$$\nabla \times \mathbf{E} = 0, \quad (3)$$

$$\nabla \cdot \mathbf{B} = 0. \quad (4)$$

where ϕ is the gravitational potential and \mathbf{F}_{vis} is the viscous force per unit volume; ρ , \mathbf{v} and P have the usual meaning of density, velocity and total pressure. By inserting into equation (3) the electric field derived from Ohm's law:

$$\mathbf{j} = \frac{1}{\eta} (\mathbf{E} + \mathbf{v} \times \mathbf{B}), \quad (5)$$

and the current density defined by Ampère's law (neglecting the displacement current):

$$\nabla \times \mathbf{B} = 4\pi \mathbf{j}, \quad (6)$$

we can reformulate the induction equation as

$$\nabla \times (\mathbf{v} \times \mathbf{B}) - \nabla \times (\eta \nabla \times \mathbf{B}) = 0. \quad (7)$$

From symmetry considerations, the magnetic field in the midplane must be

$$\mathbf{B}(z=0) = (0, 0, B_z^0), \quad (8)$$

and for the same reason (even symmetry with respect to the midplane) we define the magnetic field on the disk surface as

$$\mathbf{B}(z=H) \equiv (B_r^S, B_\phi^S, B_z^S), \quad (9)$$

$$\mathbf{B}(z=-H) \equiv (-B_r^S, -B_\phi^S, B_z^S). \quad (10)$$

For our present purpose we do not require the detailed behavior of the magnetic field within the disk; we therefore assume as a reasonable approximation for the height-averaged value above the midplane:

$$\langle \mathbf{B} \rangle_{+z} = (\frac{1}{2} B_r^S, \frac{1}{2} B_\phi^S, B_z^S). \quad (11)$$

We also approximate

$$(\partial B_r / \partial z) \simeq B_r^S / H, \quad (12)$$

$$(\partial B_\phi / \partial z) \simeq B_\phi^S / H, \quad (13)$$

$$(\partial B_z / \partial z) \simeq 0. \quad (14)$$

It can be shown that equation (14), valid to first order in H/R , follows from the solenoidal condition (4) on the magnetic field. We also assume that the upward mass flux ρv_z within the disk is negligible, that is,

$$v_z(z) \simeq 0, \quad |z| \leq H, \quad (15)$$

although v_z becomes important in the wind region above and below the disk. Consistently, we assume that the density and the mass-loss rate in the wind are negligible compared to the density and the accretion rate in the disk. Finally, we introduce a somewhat similar notation to NY94 for an easy comparison, defining $R \equiv r/r_g$, and using v and ρ as dimensionless, height-averaged radial velocity and density.

We can now rewrite the height-averaged continuity, radial momentum and azimuthal momentum equations in the form

$$\frac{d}{dR} \dot{M} = \frac{d}{dR} (-4\pi \rho R H v) = 0, \quad (16)$$

$$v \frac{dv}{dR} = (\Omega^2 - \Omega_k^2) R - \frac{1}{\rho} \frac{d}{dR} (\rho c_s^2) - \frac{1}{\rho R^2} \frac{d}{dR} \times \left[\frac{R^2 (B_\phi^S)^2}{32\pi} \right] + \frac{B_z j_\phi}{\rho}, \quad (17)$$

$$v \frac{d}{dR} (\Omega R^2) = \frac{1}{\rho R H} \frac{d}{dR} \left(R^2 v \rho H R \frac{d\Omega}{dR} \right) + \frac{B_r^S}{16\pi \rho} \frac{d}{dR} (R B_\phi^S) + \frac{B_z B_\phi^S}{4\pi \rho} \frac{R}{H}. \quad (18)$$

The vertical momentum equation is, with $v_z = 0$ and the choice of a Newtonian potential justified by the fact that our simple self-similar solutions will in any case be valid only sufficiently far away from the horizon:

$$\frac{\partial}{\partial z} \left[-\frac{GM}{(R^2 + z^2)^{1/2}} \right] = -\frac{1}{\rho(z)} \frac{\partial}{\partial z} \left[P(z) + \frac{B_\phi^2(z)}{8\pi} \right] - \frac{B_r(z) j_\phi(z)}{\rho(z)}. \quad (19)$$

We assume that only the gas pressure contributes to P , thus neglecting radiation pressure and a further magnetic pressure term produced by microscopic, isotropically tangled fields confined to the disk (see Narayan & Yi 1995b for a treatment of these terms):

$$P = P_g = \rho c_s^2, \quad (20)$$

where c_s is the isothermal sound speed ($c_s^2 \propto T$).

Finally, the cylindrical components of the current density are defined by (see eq. [6])

$$j_\phi = \frac{1}{4\pi} \left(\frac{\partial B_r}{\partial z} - \frac{\partial B_z}{\partial R} \right) \simeq \frac{1}{4\pi} \left(\frac{B_r^S}{H} - \frac{dB_z}{dR} \right), \quad (21)$$

$$j_r = \frac{1}{4\pi} \frac{\partial B_\phi}{\partial z} \simeq \frac{B_\phi^S}{H}, \quad (22)$$

$$j_z = \frac{1}{4\pi r} \frac{\partial}{\partial r} (rB_\phi), \quad (23)$$

and from the toroidal component of the induction equation we have

$$j_\phi \simeq -\frac{vB_z}{4\pi\eta}. \quad (24)$$

Using, as usual, Shakura-Sunyaev's α parameter, we take the kinematic coefficient of shear viscosity $\nu = \alpha c_s H$, and we assume the existence of a uniform turbulence (see, e.g., Lovelace, Romanova, & Bisnovatyi-Kogan 1995), so that for the magnetic diffusivity

$$\eta = \nu \quad (25)$$

Notice that, in the absence of the large-scale magnetic field, equations (16), (17), and (18) coincide with NY94's equations (1), (2), and (3), and equation (19) is reduced to $H = c_s \cdot (GM/R^3)^{-1/2} = c_s/\Omega_K$ if it is vertically averaged in the usual sense. The corresponding expression for the scale height H in presence of the magnetic field will be derived at the end of § 3.

Given a model for B , we can find self-similar solutions for H , ρ , v , Ω , and c_s^2 by solving equations (16), (17), (18), and (19) together with the energy equation (see again NY94, eq. [4]):

$$\begin{aligned} 2\rho H v T \frac{ds}{dR} &= \left(\frac{3+3\epsilon}{2}\right) 2\rho H v \frac{d(c_s^2)}{dR} - 2c_s^2 H v \frac{d\rho}{dR} \\ &= Q_{\text{vis}}^+ + Q_m^+ - Q^- \\ &= f(R)Q^+ \\ &= f v \left[2\rho H R^2 \left(\frac{d\Omega}{dR}\right)^2 + 2H \cdot 4\pi |j|^2 \right], \end{aligned} \quad (26)$$

where, in accordance to the definitions in NY94: s is the specific entropy; Q_{vis}^+ is the thermal power generated per unit area of the disk by viscous dissipation; Q_m^+ is the power dissipated by electric currents induced in the disk (Ohmic dissipation), not included in the NY94 model; Q^- is the total energy reemitted per unit time and area; $\epsilon = (5/3 - \gamma)/(\gamma - 1)$, where γ is the ratio of specific heats; f measures the degree of advection ($0 < f < 1$). We will use $\epsilon' \equiv \epsilon/f$ to parameterize the models, following NY94.

3. A MODEL FOR THE MAGNETIC FIELD

As shown in the Appendix, we look for a self-similar solution of the form

$$\begin{aligned} v \propto R^{-1/2}, \quad \Omega \propto R^{-3/2}, \quad c_s^2 \propto R^{-1}, \quad \rho \propto R^{-3/2}, \\ H \propto R, \quad B_r \propto R^{-5/4}, \quad B_z \propto R^{-5/4}, \quad B_\phi \propto R^{-5/4}. \end{aligned} \quad (27)$$

We expect $H < R$ and we drop from the equations all terms of order $(H/R)^2$, but, unlike the thin-disk approximation, we shall include terms $\sim H/R$. We shall later check this assumption by plotting the angle $\chi \equiv \arctan(H/R)$ (dotted line in Fig. 2 below). For the parameter range considered here, $\chi \lesssim 20^\circ$, that is, $H/R \lesssim 1/3$.

In the wind region, we assume (see LPP94) that the poloidal component of the field decreases along the field lines as

$$B_p(R) \equiv (B_r^2 + B_z^2)^{1/2} \sim R^{-\delta}, \quad (28)$$

with $\delta \geq 1$. The matter will leave the surface of the disk with negligible poloidal velocity and a density much lower than the value at midplane. It will then travel along the poloidal field line emerging from the point where the gas leaves the disk, and it will be centrifugally accelerated (slingshot effect) until it reaches the Alfvén speed at the cylindrical radius R_A (Alfvénic point), with a density ρ_A and a poloidal velocity

$$v_p(R_A) = \frac{B_p(R_A)}{(4\pi\rho_A)^{1/2}} \equiv v_A. \quad (29)$$

We also assume that the results derived by Mestel & Spruit (1987) in the case of a centrifugal wind from a rotating star are applicable to our problem, because of the similar (centrifugal) nature of the wind. Therefore, the poloidal velocity of the escaping wind material is, on the Alfvén surface,

$$v_p(R_A) \simeq \frac{2\sqrt{6}}{9} \Omega(R)R_A, \quad (30)$$

where $\Omega(R)$ is the angular velocity the same element of gas had when it left the disk at cylindrical radius R . It can be assumed that beyond the Alfvén surface the gas effectively conserves its angular momentum to infinity (see Mestel 1968; Weber & Davis 1967).

Moreover, the mass loss in the wind per unit magnetic flux tube, defined as

$$\eta_w \equiv \frac{\rho_w v_{p,w} S}{B_p S} = \frac{\rho_w v_{p,w}}{B_p}, \quad (31)$$

is a constant along each flux tube (S represents here the cross section of a given flux tube; ρ_w and $v_{p,w}$ are density and poloidal velocity of the wind). If $\chi = \arctan(H/R)$ is the angle between the disk surface and the plane $z = 0$, and if the field lines are inclined at an angle ψ from the z -axis (see Fig. 1), the mass-loss rate per unit area from one surface of the disk at radius R is

$$\dot{m}_w(R) = \rho_w^{(0)} v_{p,w}^{(0)} \cos(\psi + \chi), \quad (32)$$

where $\rho_w^{(0)}$ and $v_{p,w}^{(0)}$ are the initial density and poloidal velocity of the wind at the base of the corona ($\rho_w^{(0)} \ll \rho$). They are



FIG. 1.—Schematic geometry of the accretion disk and of the magnetic field lines in our self-similar model.

related to the same quantities at the Alfvénic point by virtue of equations (28), (31), and (32):

$$\rho_w^{(\circ)} v_{p,w}^{(\circ)} R^\delta \equiv \frac{\dot{m}_w(R)}{\cos(\psi + \chi)} R^\delta = \rho_A v_A R_A^\delta. \quad (33)$$

In the spirit of self-similar approximations, we shall take the angle ψ to be the same at all radii. We now need to insert the value of the magnetic field. From dimensional considerations, we have already shown (see Appendix) that self-similar solutions exist if $B^2 \sim R^{-5/2}$ in the disk; this scaling is compatible with the behavior along the field lines given in equation (28). We choose to parameterize the magnetic energy density on the disk surface as a fraction of the thermal energy density:

$$|B^S|^2 = (B_p^S)^2 + (B_\phi^S)^2 \equiv 8\pi\beta\rho c_s^2. \quad (34)$$

If $\beta = 1$ the magnetic pressure on the surface of the disk is equal to the height-averaged thermal pressure. Numerical simulations (Hawley, Gammie, & Balbus 1995; Brandenburg et al. 1995) suggest that the equipartition assumption ($\beta \simeq 1$) may be justified for a magnetic field created by a dynamo process in the disk.

From the induction equation, applied on the surface of the disk,

$$vB_z = -v \left(\frac{B_r^S}{H} - \frac{dB_z}{dR} \right) \quad (35)$$

(see eqs. [21], [24], and [25]); and given the inclination angle ψ ,

$$B_r^S = B_p^S \sin \psi \quad (36)$$

$$B_z^S = B_p^S \cos \psi. \quad (37)$$

Finally, we assume $R_A^2 \gg R^2$, so that the toroidal component of the magnetic field is given by (see Mestel 1968; Li 1992; LPP94)

$$\begin{aligned} B_\phi^S(R) &\simeq -\frac{4\pi}{R} \eta \Omega(R) R_A^2 = -\frac{4\pi}{R} \frac{\rho_w v_{p,w}}{B_p} \Omega(R) R_A^2 \\ &= -\frac{4\pi}{R} \frac{\dot{m}_w}{B_p^S \cos(\psi + \chi)} \Omega(R) R_A^2, \end{aligned} \quad (38)$$

where equation (33) has been used for the last equality.

Summing up, from equations (28), (29), (30), (31), and (33) we obtain the following system of equations:

$$\eta_w = \frac{B_p(R_A)}{4\pi v_A}, \quad (39)$$

$$R_A = \frac{9}{2\sqrt{6}} \frac{v_A}{\Omega(R)}, \quad (40)$$

$$B_p(R_A) = \left(\frac{R}{R_A} \right)^\delta B_p^S, \quad (41)$$

$$\rho_A = \frac{\dot{m}_w(R)}{v_A \cos(\psi + \chi)} \left(\frac{R}{R_A} \right)^\delta. \quad (42)$$

Equations (39), (40), (41), and (42) allow us to express R_A , ρ_A , v_A , and $B_p(R_A)$ as a function of four quantities: the poloidal field on the disk surface, B_p^S ; the mass-loss rate, \dot{m}_w ; the inclination angle of the field line, ψ ; the angular velocity of the disk at the footpoint of the field line, Ω . Making use of

equations (39), (40), and (41) we can recast equation (38) in the useful form:

$$B_\phi^S(R) = -\left(\frac{3}{2} \right)^{3/2} B_p^S \left(\frac{R}{R_A} \right)^{\delta-1}. \quad (43)$$

Then, the system of four independent equations (34), (35), (36), and (43) gives the inclination angle and the three components of the magnetic field on the disk surface, at each radius, as a function of \dot{m}_w , and of the five self-similar quantities v , Ω , ρ , c_s , H . These latter five unknowns are the solutions of the five equations (16), (17), (18), (19), and (26). At this point our model contains four free parameters (ϵ , f , δ , and β) and a physical quantity, namely the mass-loss rate \dot{m}_w , that we have not yet expressed in terms of the other variables.

Before proceeding, we need to derive a few general results. Equation (18) tells us that the specific angular momentum of the infalling matter is changed because of three effects: shear viscosity (first term on the right-hand side), which transports angular momentum outward within the disk; the centrifugal wind (third term on the right-hand side), which extracts angular momentum from the disk; and a contribution from a negative magnetic stress $\sim (B_r B_\phi/4\pi)$ (middle term), which tends to convey angular momentum toward the inner disk, but it can be shown to be numerically less important than the term responsible for the wind loss. Making use of equations (37) and (38), we see that for $\psi > \chi$ the third term on the right-hand side in the angular momentum equation (18) (i.e., the magnetic torque per unit mass due to the wind) can be rewritten in the equivalent form:

$$\frac{B_z B_\phi^S R}{4\pi\rho H} = -\frac{\dot{m}_w \cos \psi}{\rho H \cos(\psi + \chi)} \Omega R_A^2. \quad (44)$$

With a generic value for the parameter δ (an index of how much the poloidal component of the field lines is bent outside the disk), we obtain the following expressions for the Alfvén (cylindrical) radius, the magnetic field on the disk surface, and the dominant term of the magnetic torque per unit volume:

$$R_A = \left(\frac{3}{2} \right)^{3/[2(\delta+1)]} \left[\frac{\cos(\psi + \chi)}{4\pi\dot{m}_w \Omega} \right]^{1/(\delta+1)} (B_p^S)^{2/(\delta+1)} R^{\delta/(\delta+1)}, \quad (45)$$

$$\begin{cases} B_\phi^S = -\left(\frac{3}{2} \right)^{3/(\delta+1)} \left[\frac{4\pi\dot{m}_w \Omega R}{\cos(\psi + \chi)} \right]^{(\delta-1)/(\delta+1)} (B_p^S)^{(3-\delta)/(\delta+1)}, \\ (B_\phi^S)^2 + (B_p^S)^2 = 8\pi\beta\rho c_s^2, \end{cases} \quad (46)$$

$$\begin{aligned} T_m &= -\left(\frac{3}{2} \right)^{3/(\delta+1)} \frac{1}{H} \left(\frac{1}{4\pi} \right)^{2/(\delta+1)} \\ &\quad \times \cos \psi [\cos(\psi + \chi)]^{(1-\delta)/(\delta+1)} \\ &\quad \times (\dot{m}_w \Omega)^{(\delta-1)/(\delta+1)} (B_p^S)^{4/(\delta+1)} R^{2\delta/(\delta+1)}. \end{aligned} \quad (47)$$

The value of \dot{m}_w flowing out in the wind is probably the most uncertain quantity: if we follow the assumption of a locally isothermal disk [$\rho(z) \sim \rho(z=0) \exp(-z/H)^2$], as in LPP94, extending up to the region where the wind originates, the mass-loss rate would be either zero (no wind at all) for $\psi \lesssim 30^\circ$, or, for $\psi \gtrsim 30^\circ$:

$$\dot{m}_w \sim \rho(z=H) c_s \sim \rho c_s. \quad (48)$$

The latter is too large a value, clearly unphysical, as the authors point out, because the mass lost in the outflow would be larger than the mass accreted: if a disk existed, it would totally evaporate on a timescale $\sim 1/\Omega$. In the case of LPP94's inviscid, thin, quasi-Keplerian disk, with $\delta > 1$, there appears to be no stable solution allowing for a reasonably small but finite value of \dot{m}_w , because $\delta \dot{m}_w / |\delta v_r| > 0$, $\delta |v_r| / \delta \psi > 0$ and $\delta \psi / \delta \dot{m}_w > 0$. In other words, if one started with a low mass-loss rate, and with a field angle $\psi \simeq 30^\circ$ (for which we expect the mass loss to be very small), one would end up either with the upper limit for \dot{m}_w given by equation (48) and with the field bent parallel to the disk surface ($\psi \simeq 90^\circ$), or with the field close to the vertical axis and no wind at all being launched.

In fact, as we have assumed, it is more likely that the wind starts from a corona, not from the upper layer of an isothermal disk. Therefore, we assume that the mass-loss rate is proportional to the density at the base of the corona, which is likely to be a few orders of magnitude smaller than the density near the upper surface of the disk (the density drops sharply at the disk-corona interface, whereas the temperature increases, so that $\rho(z)c_s^2(z)$ is approximately a continuous function). The density and the sound speed in the corona may be related to the corresponding quantities near the disk surface, for example through nonthermal processes such as mechanic heating, but it is not our purpose here to investigate this relation. In our model, which includes viscosity and advection, the stability of the solutions is not obvious at first sight, given the number of terms that contribute to the radial and angular momentum equations. A more comprehensive analysis of this aspect of the problem is left to further work, but we stress that the mass-loss rate would in any case be negligible compared to the accretion rate, as shown by the following simple order-of-magnitude calculation. The accretion rate is given by

$$\dot{M} = -4\pi R H \rho v \sim -4\pi R^2 \rho c_s \frac{v}{v_K}, \quad (49)$$

and the total mass-loss rate in the wind by

$$2\pi R^2 \dot{m}_w \sim 2\pi R^2 \rho_w^{(\circ)} v_w^{(\circ)} = 4\pi R^2 \rho c_s \frac{v_w^{(\circ)} \rho_w^{(\circ)}}{c_s 2\rho}. \quad (50)$$

It is reasonable to assume $v_w^{(\circ)} < c_{s,w}^{(\circ)} \sim c_s$, with $c_{s,w}^{(\circ)}$ denoting the sound speed of the wind at the base of the corona, and $\rho_w^{(\circ)} \ll \rho$, so that

$$\frac{v_w^{(\circ)} \rho_w^{(\circ)}}{c_s 2\rho} \ll \left| \frac{v}{v_K} \right|, \quad (51)$$

especially if we drop the hypothesis of a locally isothermal disk and allow for the temperature in the midplane to be higher than that on the disk surface (for the range of parameters we are dealing with in the case of advective disks, $|v/v_K| \sim 10^{-3} - 10^{-1}$). This justifies our assumption of $2\pi R^2 \dot{m}_w \ll \dot{M}$.

Furthermore, unlike LPP94, we assume $\delta = 1$ as a reasonable approximation for inclination angles larger than 30° ($B_p \sim R^{-1}$ along each field line) in the context of self-similar solutions; each field line is in this limiting case a conical helix (outside the disk). We can justify this approximation by noting that the magnetic pressure generated by the poloidal magnetic field is assumed to be stronger than the thermal pressure in the lower layer of the corona, where

the wind starts (where $B^2 \sim \rho c_s^2 \gg \rho_w c_{s,w}^2$), and we shall verify that the Alfvén point for a given field line is located at a much larger radius than the footpoint of that line on the disk surface ($R_A^2 \gg R^2$). This suggests that the poloidal field can be considered approximately rigid near the disk surface, almost up to the Alfvén surface. Further away from the disk, toward the Alfvén point, wind effects tend to lift the poloidal field perpendicularly to the disk, finally collimating the field lines toward the z -axis (e.g., Ostriker 1997).

An important consequence of our choice of $\delta = 1$ is that the loss of angular momentum, the radial velocity of the accretion flow and all the disk equations are then independent of the mass-loss rate in the wind; the magnetic torque per unit volume is simply

$$T_m \simeq -\left(\frac{3}{2}\right)^{3/2} \frac{1}{H} \left(\frac{\cos \psi}{4\pi}\right) (B_p^S)^2 R. \quad (52)$$

Physically, a more tenuous wind (smaller \dot{m}_w) will reach the Alfvén point at a larger cylindrical radius, i.e., with a larger lever arm R_A , and will carry away a larger amount of angular momentum per unit mass, so that these two effects balance each other. Our simple model breaks down when the wind and therefore also the magnetic torque drop altogether, for $\psi \lesssim 30^\circ$.³

In the limits of validity of our assumption we can derive the three components of the magnetic field, from equations (36), (38), (39), and (45):

$$\begin{aligned} B_\phi^S &= -\left(\frac{3}{2}\right)^{3/2} B_p^S, \\ B_r^S &= B_p^S \sin \psi, \\ B_z^S &= B_p^S \cos \psi. \end{aligned} \quad (53)$$

$$\begin{aligned} (B_\phi^S)^2 &= \frac{27}{35} (8\pi\beta) \rho c_s^2, \\ (B_r^S)^2 &= \frac{8}{35} (8\pi\beta \sin^2 \psi) \rho c_s^2, \\ (B_z^S)^2 &= \frac{8}{35} (8\pi\beta \cos^2 \psi) \rho c_s^2. \end{aligned} \quad (54)$$

For simplicity of notation, we will drop the superscript S henceforth, when referring to the field at the disk-wind interface.

We can now insert these values for the magnetic field into equations (19) and (34), and take a height average. The scale height of the disk and the inclination angle from the z -axis of the field lines outside the disk are given (in implicit form) by

$$\frac{H}{R} \simeq \frac{c_s}{v_K} \left[1 - \left(\frac{27}{35} - \frac{8}{35} \frac{v}{\alpha c_s} \sin \psi \cos \psi \right) \beta \right]^{1/2}, \quad (55)$$

$$\tan \psi = -\frac{v}{\alpha c_s} - \frac{5H}{4R}. \quad (56)$$

Finally, we check that our assumption of $R_A^2 \gg R^2$ is correct, as long as the mass-loss rate in the wind is negligible compared to \dot{M} ; from equations (45) and (50) we see that

$$R_A^2 \sim \beta \frac{\rho c_s}{\rho_w v_w} \frac{c_s}{v_K} R^2 \sim \beta \frac{\dot{M}}{4\pi R^2 \dot{m}_w} \frac{c_s}{v} R^2 \gg R^2, \quad (57)$$

provided the field (β) is not too weak.

³ The value $\psi \lesssim 30^\circ$ as the minimum angle to launch a wind is calculated by balancing the gravitational and centrifugal forces along a poloidal field line above the disk (see, e.g., Blandford & Payne 1982). This value may be different in advective disk models, where the rotation of the disk surface can be sub-Keplerian and the thermal pressure can become important.

4. RESULTS AND DISCUSSION

The set of MHD equations in self-similar form defined in § 3 and explicitly written in the Appendix can be solved numerically with Newton's method. In the limit of $\beta \rightarrow 0$ they admit an analytical solution derived by NY94. The first significant effect of the magnetic field on the disk structure is what we can call a squeezing effect: the toroidal magnetic pressure gradient in the disk counterbalances the thermal pressure gradient. As a consequence, the scale height H is reduced compared to the nonmagnetic case (see Lovelace et al. 1995). In the self-similar approximation the thickness of the disk is simply modeled by the angle $\chi = \arctan(H/R)$ (see Fig. 1). At the same time, the magnetic field lines form an angle ψ with the vertical axis, determined by the dragging of the field in the disk by the accreting matter. Qualitatively speaking, the stronger the magnetic field, the higher the radial velocity of the inflowing matter and, as a consequence, the larger ψ , in accordance with the result obtained by Lubow et al. (1994a, 1994b) in the case of a thin, inviscid disk. In order for the wind to exist, we require $30^\circ \lesssim \psi < (90 - \chi)$, namely, our model breaks down when the dragging is so strong that the field plunges into the disk. This may happen when the magnetic pressure on the surface is more less in equipartition with the height-averaged gas pressure ($B^2 \simeq 8\pi\rho c_s^2$). We note that the disk is possibly disrupted at that point. It may also happen for much lower values of the magnetic field ($\beta \lesssim 0.1$) in two physical regimes: for highly advective (therefore thick and with high radial velocity) disks, characterized by $\epsilon' \lesssim 1$; and for low values of α , implying (for the uniform turbulence approximation) low diffusivity η , meaning that the field is easily dragged by the inflow. Some numerical calculations of the inclination angle and of the thickness of the disk as a function of β for different values of α and ϵ' are shown in Figure 2. Notice that we find no reason to impose a maximum inclination angle, apart from the requirement that the field be emerging from the disk, unlike the assumption made in Li (1995). This is mainly due to the fact we assume a much lower value of the diffusivity η (a factor of $\sim 1/\alpha$ smaller), and as a consequence the field lines in our model are more easily bent toward the disk surface.

The behavior of some height-averaged disk quantities is plotted in Figures 3 and 4; we see as particularly significant the increase in the inward radial velocity of the accreting matter (for $\beta = 0$ we reobtain of course the analytical expressions calculated in NY94). The relation between increased loss of angular momentum (via the magnetized wind) and increased radial velocity (in absolute value) is consistent with the results of LPP94 and with what we can qualitatively expect from simple physical considerations: the faster the accreting matter can get rid of its angular momentum, the faster it can flow inward. On the one hand, the squeezing effect of the large-scale magnetic field counterbalances the thickening of the disk generated by advection. On the other hand, the magnetized wind reinforces their high radial velocity, a feature of advective disks. The height-averaged sound speed tends to decrease in our self-similar model. This may be related to the limited role played by the viscous shear in transporting angular momentum outward and it corresponds to a decrease of the coefficient of kinematic viscosity ν , leading to a lower viscous heating. We also notice that the gas pressure ρc_s^2 is almost independent of the degree of advection for higher

values of β . Moreover, for $\beta \gtrsim 0.2$ the gas pressure is also approximately independent of the magnetic field. This happens because the density ρ is increased by the squeezing effect, while the temperature $T \propto c_s^2$ is correspondingly lower, in solutions with a larger magnetic parameter β . This is consistent with the fact that the magnetic field is doing work to accelerate the wind. Ultimately, the only source of energy is the drop in the gravitational potential of the accreting matter, and we can expect that the work done by the magnetic field is at the expense of the fraction of energy heating the gas.

The effectiveness of the centrifugal wind in removing angular momentum, compared with the viscous shear, is shown in Figure 5, again for high, intermediate and low degrees of advection, and high and low viscosity. The total specific angular momentum lost in unit time by an element of gas can increase by a factor 2 to 4 with respect to the rate in the absence of a centrifugal wind, but the fraction of angular momentum transported outward by the viscous torque becomes immediately (already for $\beta \sim$ a few times 10^{-2}) negligible compared to the fraction lost in the wind. It appears that a centrifugal wind is a much more efficient way to remove angular momentum from the accreting matter, to the point that we can almost neglect the viscous torque in the angular momentum equation. For a given value of the magnetic field, we can include the loss of angular momentum due to the wind in an effective viscosity parameter α_{eff} defined by

$$v \frac{d}{dR} (\Omega R^2) = \frac{\alpha_{\text{eff}}}{\rho R H} \frac{d}{dR} \left(R^3 c_s \rho H^2 \frac{d\Omega}{dR} \right), \quad (58)$$

$$\alpha_{\text{eff}} \equiv \alpha + \left[\frac{B_r^S}{16\pi\rho} \frac{d}{dR} (R B_\phi^S) + \frac{B_z B_\phi^S}{4\pi\rho} \frac{R}{H} \right] \times \left[\frac{1}{\rho R H} \frac{d}{dR} \left(R^3 c_s \rho H^2 \frac{d\Omega}{dR} \right) \right]^{-1}. \quad (59)$$

As shown in Figure 6, the onset of a magnetically driven wind produces a dramatic increase of the effective viscosity parameter, which can be very high, up to ~ 1 for a large degree of advection or even $\gtrsim 10$ for a small degree of advection. This is in good agreement with the results obtained by Li (1995) for a thin, nonadvective disk, for which he finds $\alpha_{\text{eff}} \sim 30$. Notice also that α_{eff} depends very little on the value of the "true" viscosity parameter α , which can be very small.

Although investigating the behavior of the magnetic field and associated currents within the disk was not the main purpose of our work, we also notice that in the energy equation, the heating term due to viscous dissipation seems to dominate over the term from Ohmic dissipation for low and intermediate values of the magnetic field. The Ohmic dissipation gives a larger contribution for $\beta \rightarrow 1$ (Fig. 7).

A feature of self-similar solutions scaling as powers of R is that the only way to obtain a steeper gradient of the specific angular momentum ΩR^2 , as required when we increase the removal of angular momentum from the infalling matter, is to increase the angular velocity Ω . We note that in our self-similar treatment the angular velocity Ω increases with the magnetic field ($\Omega \rightarrow \Omega_K$). As a consequence, if α is kept constant, increasing the magnetized wind leads to a larger extraction of angular momentum from the disk at a certain

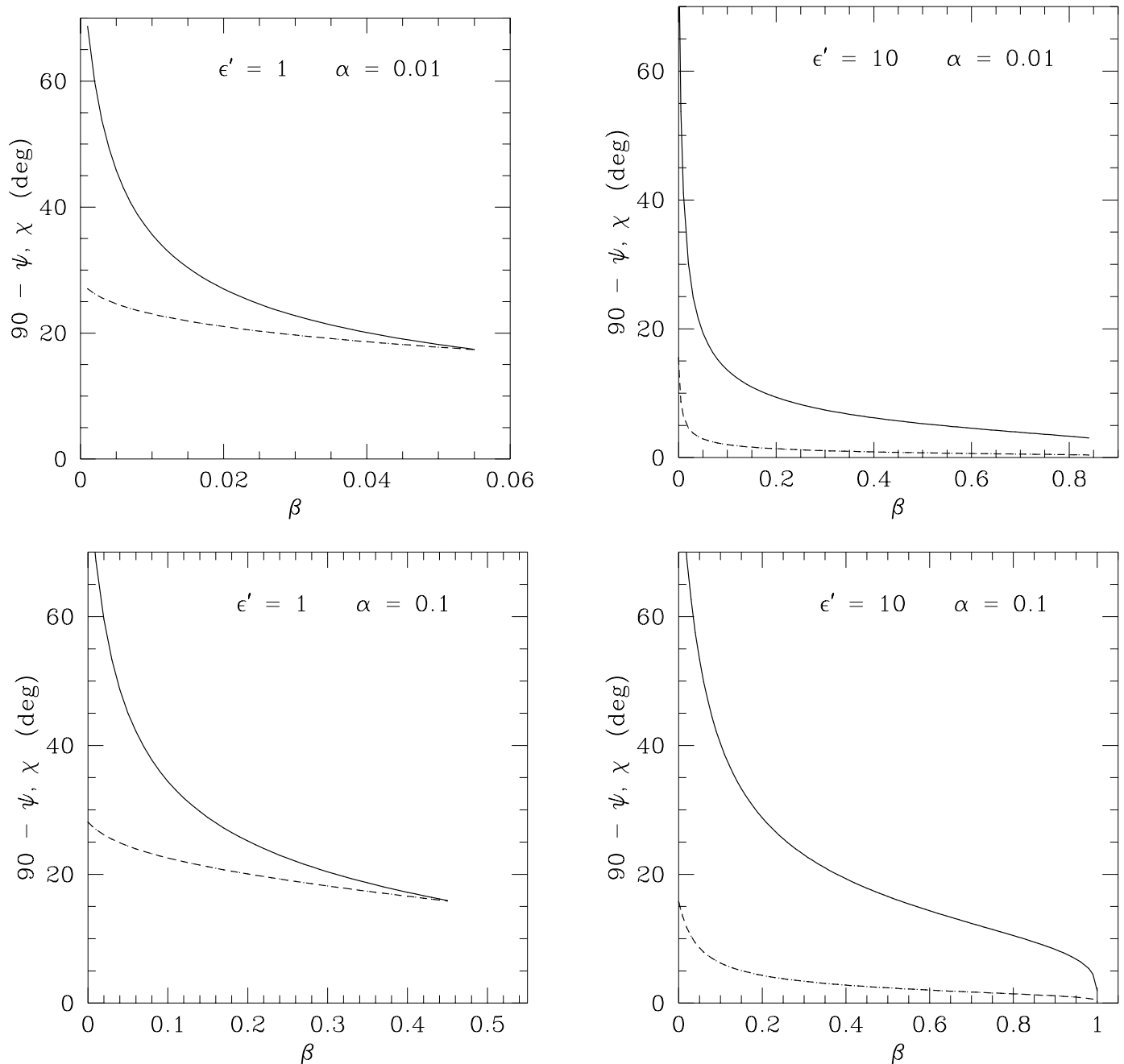


FIG. 2.—In each plot, the solid line represents the angle $90^\circ - \psi$ between the field lines and the disk midplane; the dotted line represents the angle $\chi = \arctan(H/R)$ (thickness of the disk). Our model of magnetic field is physical only when the field is above the disk, for $(90^\circ - \psi) > \chi$, and a centrifugal wind can only be launched for $(90^\circ - \psi) \lesssim 60^\circ$. The parameter β is defined as $B_{\text{out}}^2/(8\pi\rho c_s^2)$. The two upper plots refer to a low value of viscosity, whereas the lower plots are drawn for high viscosity. The parameter ϵ' indicates the degree of advection in the disk: $\epsilon' = 1$ characterizes a predominantly advective disk, while $\epsilon' = 10$ indicates a low degree of advection. Highly advective and highly viscous disks tend to be thicker; on the other hand, disks with low viscosity drag the magnetic field inward more easily, and the field lines are in fact more bent toward the disk surface.

radius. The self-similar behavior of the angular momentum gradient is shown in Figure 7. As to the radial velocity, using a self-similar approximation scaling as $v \sim R^{-1/2}$ corresponds to fixing the radial velocity on the outer boundary as $v_{\text{out}} \simeq 0$ and changing the value on the inner boundary according to the physical conditions encountered in the disk.

5. CONCLUSIONS

The main purpose of this paper was to show the effect of a large-scale magnetic field (with open field lines) threading

an accretion disk, and the importance of a magnetized, centrifugally driven wind as a way to transport angular momentum outward. We solved the magnetohydrodynamic equations self-consistently for the disk and the magnetic field structure, using height-averaged quantities in describing the disk structure, and a self-similar approximation, which can provide us with at least a qualitative indication of the behavior of the system not too close to the boundaries; these equations reduce to the advective disk equations extensively studied by Narayan & Yi (1994, 1995a, 1995b) in the case of vanishing magnetic field, and to the

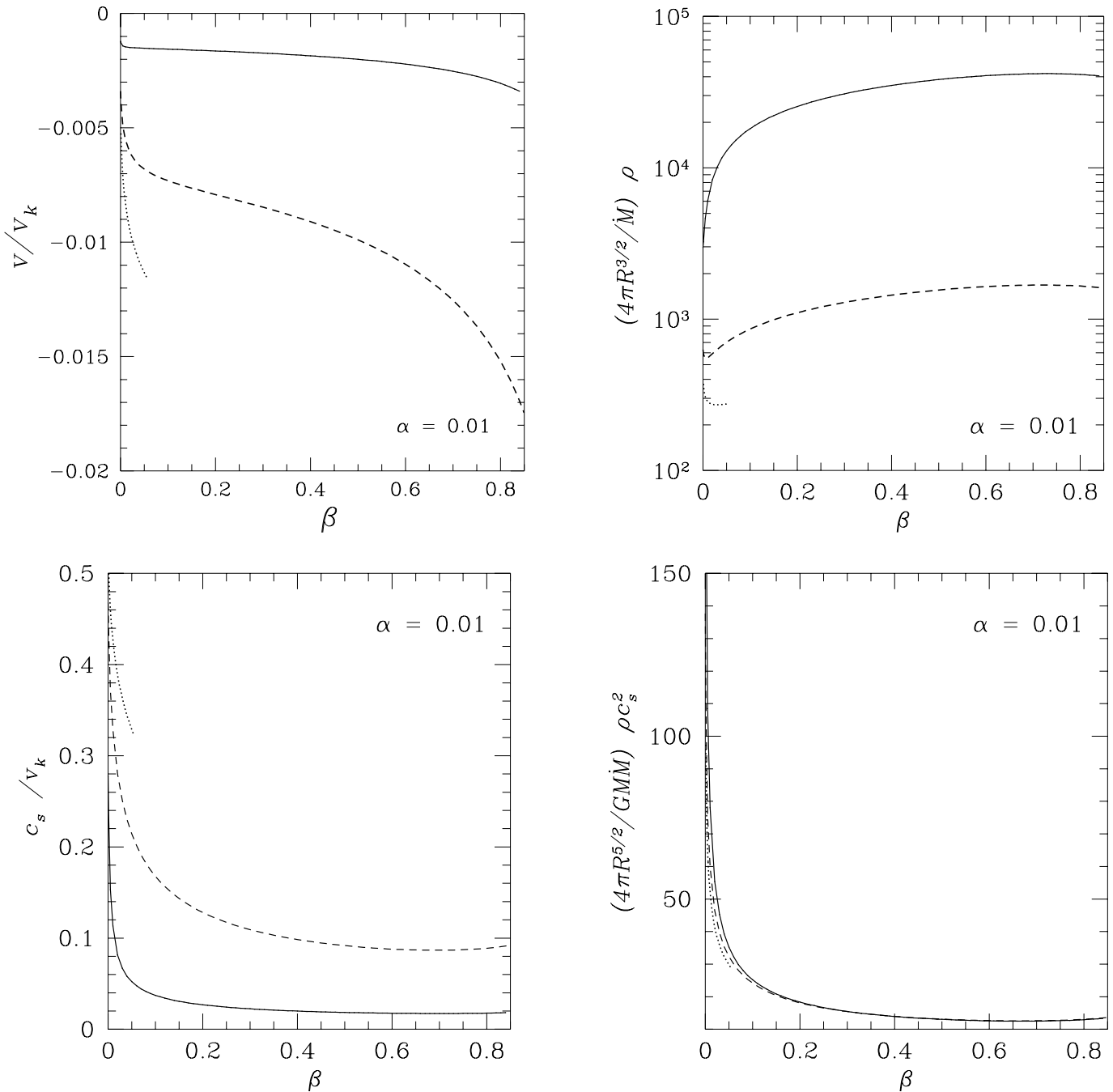


FIG. 3.—Some height-averaged physical quantities for the disk, as a function of the magnetic parameter β , for $\alpha = 0.01$ (low viscosity). In each plot, the solid line refers to $\epsilon' = 10$ (low degree of advection), the dashed line to $\epsilon' = 2$ (moderate degree of advection), and the dotted line to $\epsilon' = 10$ (high degree of advection). A classical Shakura-Sunyaev disk would have $\epsilon' \rightarrow \infty$. The plots are drawn only in the range of values for β where our model can be physical. The four quantities plotted are radial velocity v , density ρ , sound speed c_s , and gas pressure ρc_s^2 , all in dimensionless form. For $\beta \rightarrow 0$ the values calculated by NY94 are recovered.

problem discussed by LPP94 for a thin, nonadvective and nonviscous disk. We assumed the existence of a tenuous corona from which the wind is launched (therefore the mass-loss rate in the wind is negligible compared to the accretion rate), and we observed that assuming straight field lines for the poloidal field outside the disk is probably a valid approximation to the real case, and the most convenient, because the angular momentum loss rate and the toroidal magnetic field turn out to be independent of the mass-loss rate, whose value is very uncertain.

The disk structure and the field geometry are closely

linked, because the accreting matter tends to drag the field inward: radial velocity of the inflow and kinematic viscosity (equal to magnetic diffusivity in the uniform turbulence approximation) determine the inclination angle of the field lines from the vertical. Conversely, the magnetic field tends to squeeze the disk and to increase the radial velocity by removing angular momentum. A centrifugal wind seems to be a much more efficient way to transport angular momentum outward than shear viscosity. The onset of a wind extracting angular momentum from the disk can be seen as a dramatic increase of an “effective” viscosity parameter

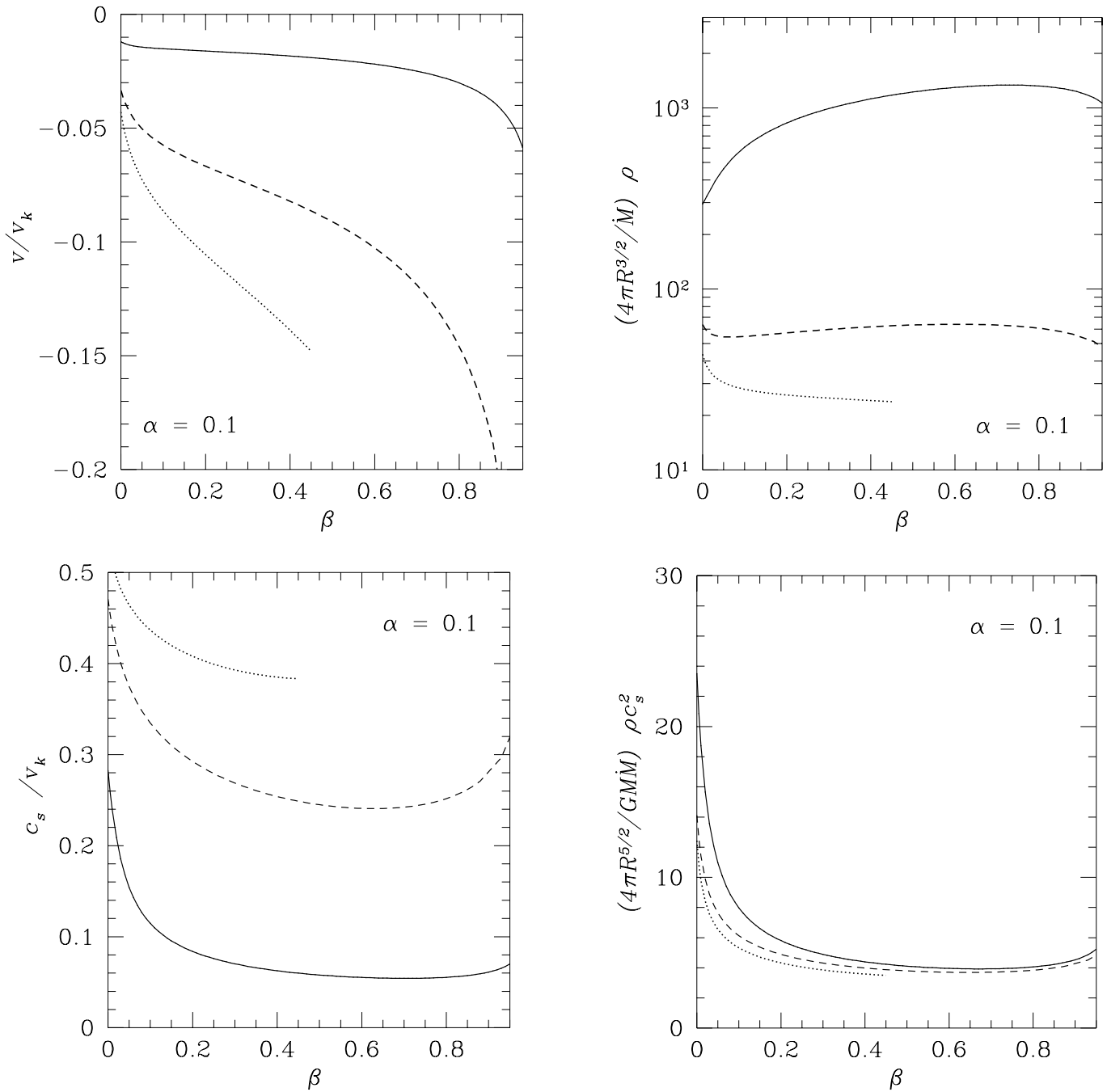


FIG. 4.—Same as Fig. 3, but in the case of $\alpha = 0.1$ (high viscosity). Solid, dashed, and dotted lines refer to $\epsilon' = 10$, $\epsilon' = 2$, and $\epsilon' = 1$, respectively, as before.

α_{eff} . Further study will require a more detailed modeling of the vertical structure of the disk and of the corona, and a

more careful treatment of boundary conditions, for which self-similar solutions may not be suitable.

APPENDIX

SELF-SIMILAR EQUATIONS

For simplicity, we are looking for self-similar solutions (valid at all radii) in which all the unknown quantities scale as powers of R in the disk:

$$v \equiv AR^\alpha, \quad \Omega \equiv \omega R^\beta, \quad c_s \equiv CR^\gamma, \quad \rho \equiv \varrho R^\delta, \quad H \equiv hR^\epsilon, \quad B_r \equiv b_r R^{\eta_1}, \quad B_\phi \equiv b_\phi R^{\eta_2}, \quad B_z \equiv b_z R^{\eta_3}. \quad (\text{A1})$$

By inserting these definitions into equations (16), (17), and (18), and by equating the exponents of R in the various terms, we

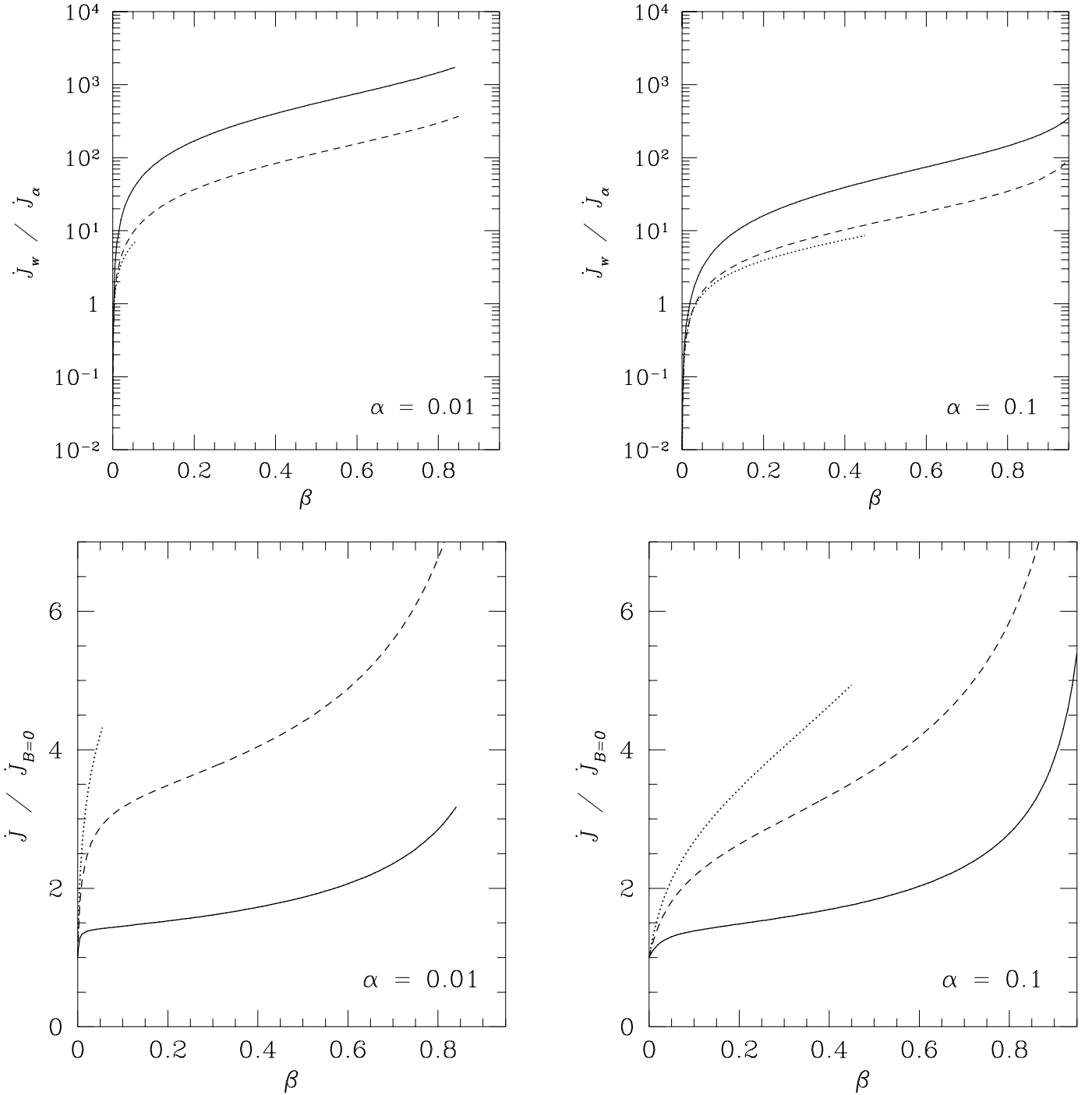


FIG. 5.—Rate of loss of the specific angular momentum of the accreting matter. The upper plots show the relative importance of the centrifugal wind and of the viscous shear for removing angular momentum: the former is much more efficient already at low values of the magnetic field, even for relatively high values of α ; solid, dashed, and dotted lines refer to $\epsilon' = 10$, $\epsilon' = 2$, and $\epsilon' = 1$, respectively, as usual. The lower plots show the total loss rate (wind plus shear) compared to the rate at $\beta = 0$ when only the viscous shear is present; the inflowing gas loses angular momentum at a rate a few times faster when the wind is present.

obtain

$$\begin{cases} \delta + 1 + \epsilon + \alpha = 0, \\ 2\alpha - 1 = 2\beta + 1 = -2 = \gamma - 1 = 2\eta_2 - \delta - 1 = \eta_3 - \delta + \eta_1 - \epsilon = 2\eta_3 - \delta - 1, \\ \alpha + \beta + 1 = \epsilon + \gamma + \beta = \eta_1 + \eta_2 - \delta = \eta_2 + \eta_3 + 1 - \epsilon - \delta. \end{cases} \quad (\text{A2})$$

By solving the system of equation (A2), one can verify that a self-similar solution exists if

$$v = AR^{-1/2}, \quad \Omega = \omega R^{-3/2}, \quad c_s = CR^{-1/2}, \quad \rho = \varrho R^{-3/2}, \quad H \equiv \tan \chi R, \quad B_i = b_i R^{-5/4}. \quad (\text{A3})$$

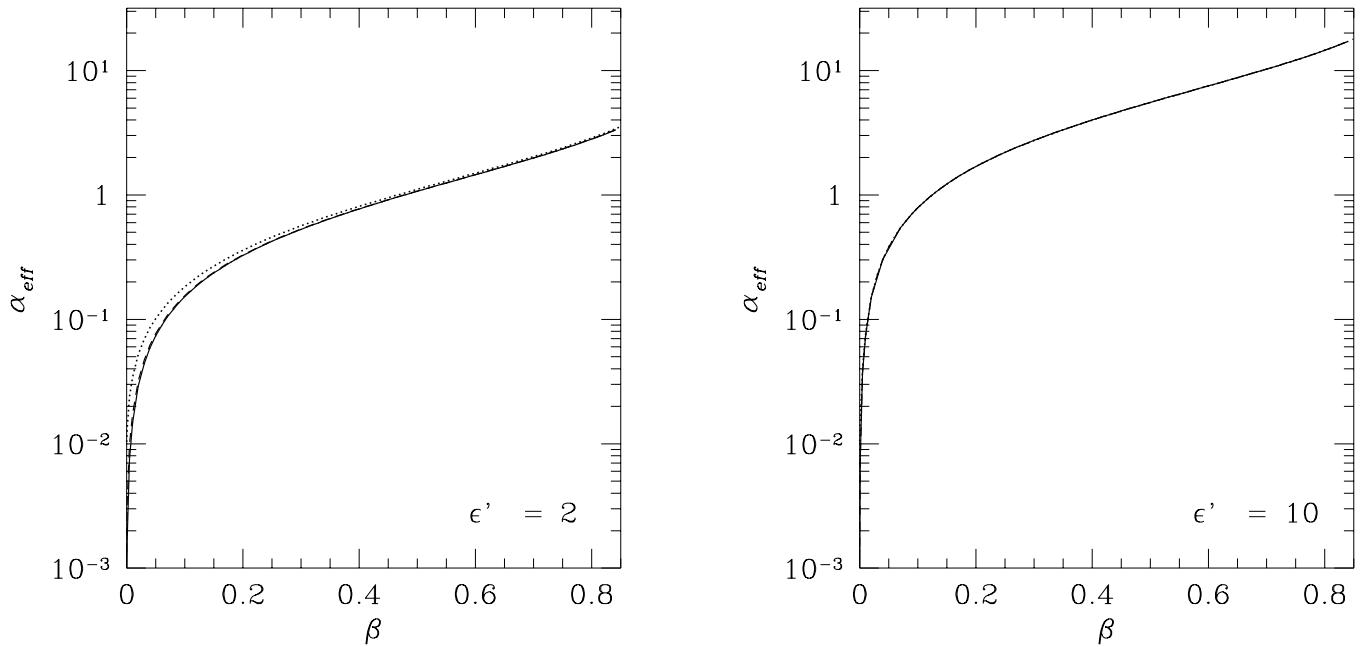


FIG. 6.—Effective value α_{eff} of the viscosity parameter as a function of the magnetic field, for two values of ϵ' ($\epsilon' = 2$ on the left and $\epsilon' = 10$ on the right). The solid, dashed, and dotted lines, almost coincident, correspond to $\alpha_{\text{vis}} \equiv \alpha = \nu/(Hc_s) = 10^{-4}$, 10^{-3} , and 10^{-2} , respectively. Regardless of the true viscosity of the disk, the loss of angular momentum in the wind can be described as being caused by a high value of α_{eff} , higher for nonadvective disks, for which Hc_s is smaller.

From the continuity equation (16) we can also derive the useful relation

$$\rho = -\frac{\dot{M}}{4\pi A \tan \chi} R^{-3/2}. \quad (\text{A4})$$

An analogous set of self-similar solutions scaling as powers of R has been adopted by Spruit et al. (1987) and by NY94, in the absence of magnetic field.

By inserting the self-similar variables defined in equations (A3) and (A4), and the magnetic field given by equations (53) and (54), into the system of MHD equations (17), (18), (26), (55), and (56), we obtain the following system of dimensionless equations, to be solved for A , ω , C , $\psi = \arctan(B_r/B_z)$ and $\chi = \arctan(H/R)$:

$$-\frac{A^2}{2} = B^2 - 1 + \frac{5}{2} C^2 - \frac{16}{35} \beta \frac{AC \cos^2 \psi}{\alpha \tan \chi} + \frac{27}{280} \beta C^2, \quad (\text{A5})$$

$$\frac{1}{2} \omega = -\frac{3}{4} \frac{\alpha C \omega}{A} \tan \chi - \frac{12\sqrt{6}}{35} \beta \frac{C^2 \cos \psi}{A \tan \chi} + \frac{3\sqrt{6}}{140} \beta \frac{C^2 \sin \psi}{A}, \quad (\text{A6})$$

$$3\epsilon' A = -\frac{9}{2} \frac{\alpha \omega^2 \tan \chi}{C} - 4\alpha\beta \frac{C}{\tan \chi} \left(\frac{27}{35} + \frac{8}{35} \sin^2 \psi \right) - \frac{16}{7} \alpha\beta C \cos \psi \sin \psi, \quad (\text{A7})$$

$$\tan \chi = C \left[1 - \left(\frac{27}{35} - \frac{8}{35} \frac{A}{\alpha C} \cos \psi \sin \psi \right) \beta \right], \quad (\text{A8})$$

$$\tan \psi = -\frac{A}{\alpha C} - \frac{5}{4} \tan \chi. \quad (\text{A9})$$

If we assume $\beta = 0$ (no magnetic field), equation (A9) cannot be defined, and the other four equations can be solved analytically. The results discussed in NY94 are recovered in this limiting case:

$$A = -(5 + 2\epsilon') \frac{g(\alpha, \epsilon')}{3\alpha} \simeq -\frac{3\alpha}{(5 + 2\epsilon')}, \quad (\text{A10})$$

$$\omega = \left[\frac{2\epsilon'(5 + 2\epsilon')g(\alpha, \epsilon')}{9\alpha^2} \right]^{1/2} \simeq \left(\frac{2\epsilon'}{5 + 2\epsilon'} \right)^{1/2}, \quad (\text{A11})$$

$$C^2 = \frac{2(5 + 2\epsilon')g(\alpha, \epsilon')}{9\alpha^2} \simeq \frac{2}{5 + 2\epsilon'}, \quad (\text{A12})$$

$$\tan \chi = C, \quad (\text{A13})$$

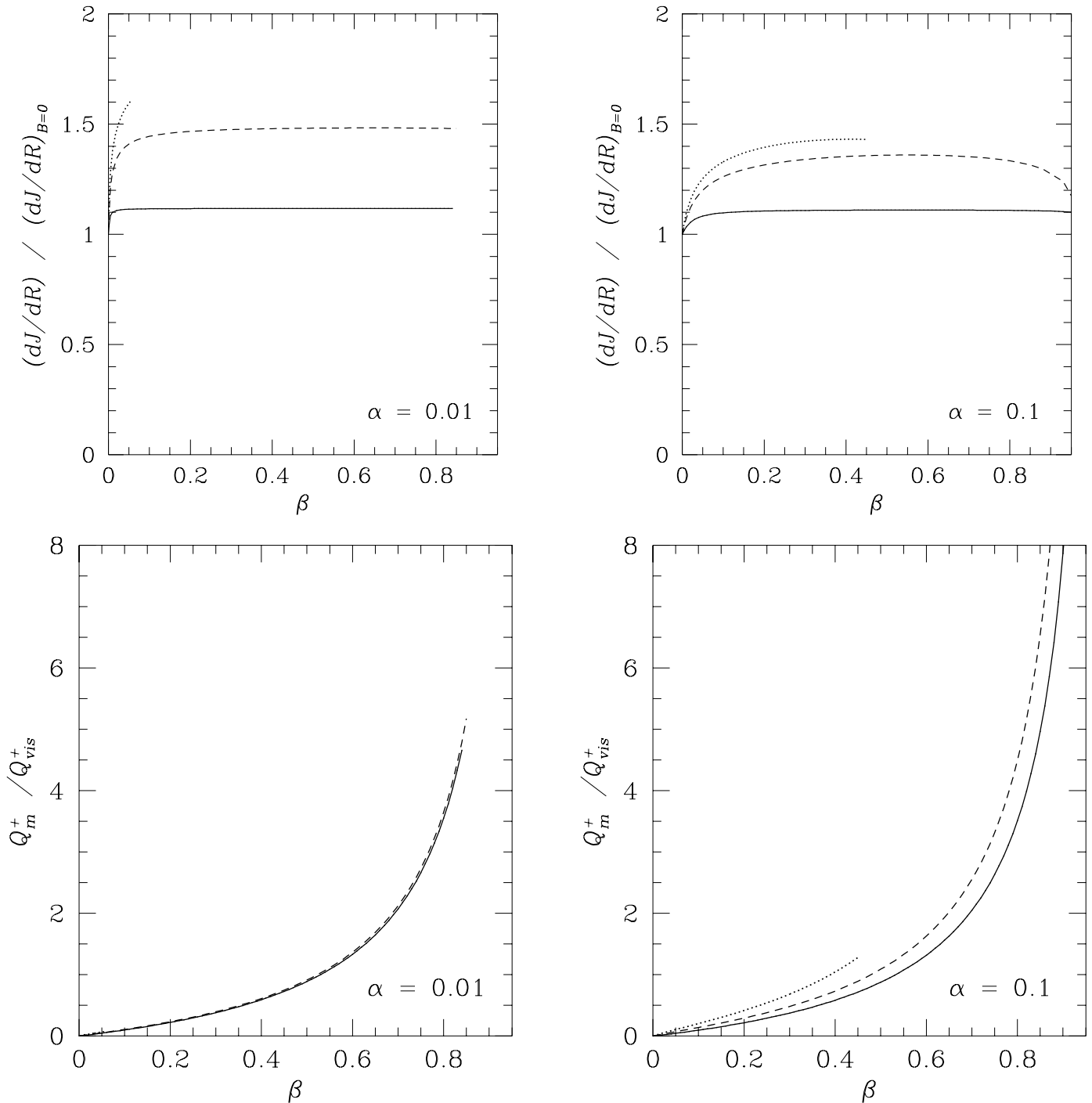


FIG. 7.—In the upper plots the specific angular momentum gradient is shown (loss of specific angular momentum per unit “ring” as the gas flows down). Again, the presence of a wind makes the gradient steeper (angular momentum is lost more quickly, as expected). The lower plots show the relative contribution of viscous and Ohmic dissipation to the heating rate within the disk. The same conventions for ϵ' are used as before.

where the second relation in equations (A10), (A11), and (A12) is approximately true for $\alpha \ll 1$, and

$$g(\alpha, \epsilon') \equiv \left[1 + \frac{18\alpha^2}{(5 + 2\epsilon')^2} \right]^{1/2} - 1. \quad (\text{A14})$$

REFERENCES

- Abramowicz, M. A., Czerny, B., Lasota, J. P., & Szuszkiewicz, E. 1988, *ApJ*, 332, 646
 Blandford R. D., & Payne, D. G. 1982, *MNRAS*, 199, 883
 Brandenburg, A., Nordlund, Å., Stein, R. F., & Torkelsson, U. 1995, *ApJ*, 446, 741
 Campbell, C. G. 1992a, *Geophys. Astrophys. Fluid Dyn.*, 63, 179
 ———. 1992b, *Geophys. Astrophys. Fluid Dyn.*, 63, 197
 Chakrabarti, S. K., & Titarchuk, L. G. 1995, *ApJ*, 465, 623; erratum, 467, 474 (1996)
 Ebisawa, K., Titarchuk, L., & Chakrabarti, S. K. 1996, *PASJ*, 48, 59
 Hawley, J. F., Gammie, C. F., & Balbus, S. A. 1995, *ApJ*, 440, 742
 Lasota, J. P., Abramowicz, M. A., Chen, X., Krolik, J., Narayan, R., & Yi, I. 1996, *ApJ*, 462, 142
 Li, J. 1992, PhD thesis, Univ. Sussex

- Li, Z.-Y. 1995, *ApJ*, 444, 848
Livio, M. 1997, in ASP Conf. 121, *Accretion Phenomena and Related Outflows*, ed. D. T. Wickramasinghe, L. Ferrario, & G. Bicknell (San Francisco: ASP), 845
Lovell, R. V. E., Romanova, M. M., & Bisnovaty-Kogan, G. S. 1995, *MNRAS*, 275, 244
Lubow, S. H., Papaloizou, J. C. B., & Pringle, J. E. 1994a, *MNRAS*, 267, 235
———. 1994b, *MNRAS*, 268, 1010 (LPP94)
Lynden-Bell, D., & Pringle, J. E. 1974, *MNRAS*, 168, 603
Mestel, L. 1968, *MNRAS*, 138, 359
Mestel, L., & Spruit, H. C. 1987, *MNRAS*, 226, 57
Murray, N., & Chiang, J. 1996, *Nature*, 382, 789
Narayan, R. 1996, *ApJ*, 462, 136
Narayan, R., McClintock, J. E., & Yi, I. 1996, *ApJ*, 457, 821
Narayan, R., & Yi, I. 1994, *ApJ*, 428, L13 (NY94)
———. 1995a, *ApJ*, 444, 231
———. 1995b, *ApJ*, 452, 710
Narayan, R., Yi, I., & Mahadevan, R. 1995, *Nature*, 374, 623
Novikov, I. D., & Thorne, K. S. 1973, in *Black Holes*, ed. C. DeWitt & B. DeWitt (New York: Gordon & Breach), 343
Ostriker, E. 1997, in ASP Conf. 121, *Accretion Phenomena and Related Outflows*, ed. D. T. Wickramasinghe, L. Ferrario, & G. Bicknell (San Francisco: ASP), 439
Shakura, N. I., & Sunyaev R. A. 1973, *A&A*, 24, 337
Spruit, H. C., Matsuda, T., Inoue, M., & Sawada, K. 1987, *MNRAS*, 229, 517
Sun, W. H., & Malkan, M. 1989, *ApJ*, 346, 68
Wardle, M., & Königl, A. 1993, *ApJ*, 410, 218
Weber, E. J., & Davis, L., Jr. 1967, *ApJ*, 148, 217